Inorganic Chemistry

Article

pubs.acs.org/IC

Controlled Growth and Applications of Complex Metal Oxide $ZnSn(OH)_6$ Polyhedra

Jingzhou Yin,[†,‡,§] Feng Gao,*[,†] Chengzhen Wei,[†,‡] and Qingyi Lu*[,‡]

[†]Department of Materials Science and Engineering, Nanjing University, Nanjing 210093, P. R. China

[‡]State Key Laboratory of Coordination Chemistry, Coordination Chemistry Institute, Nanjing National Laboratory of Microstructures, School of Chemistry and Chemical Engineering, Nanjing University, Nanjing 210093, P. R. China

[§]School of Chemistry and Chemical Engineering, Huaiyin Normal University, Huai'an 223300, P. R. China

Supporting Information

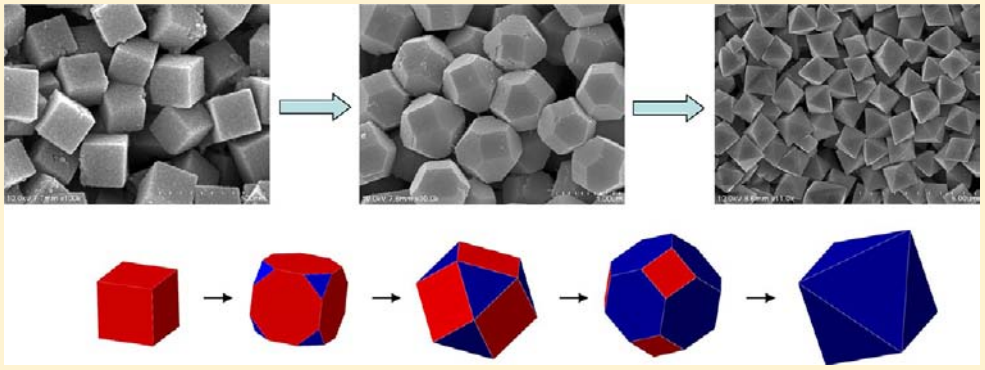

ABSTRACT: We successfully controlled the crystallographic surface of $ZnSn(OH)_6$ crystals and systematically obtained $ZnSn(OH)_6$ crystals in different shapes including cubes, truncated cubes, cuboctahedrons, truncated octahedrons, and octahedrons using a simple solvothermal method in a methylcellulose (MC) ethanol/water solution. By simply adjusting the amount of the NaOH solution added to the reaction system, we observed the shape evolution of $ZnSn(OH)_6$ particles from cube to octahedron, with the sizes gradually increasing from about 200 nm to 1−2 μm. These results not only provide $ZnSn(OH)_6$ polyhedra bound by different lattice planes, but also make it possible to investigate the morphology−property relationship of $ZnSn(OH)_6$ particles with different morphologies obtained under similar conditions. The antibacterial activities of the as-prepared $ZnSn(OH)_6$ polyhedral particles were studied. It was found that the antibacterial activities of $ZnSn(OH)_6$ particles against *Escherichia coli* depend on the shape of the $ZnSn(OH)_6$ particles, demonstrating that the surface structure of nanocrystals affects the antibacterial activity. Additionally, the obtained $ZnSn(OH)_6$ polyhedra can be applied as precursors for Zn_2SnO_4/SnO_2 composites with different morphologies by calcining at 600 °C.

INTRODUCTION

Crystalline materials with definite crystal planes generally exhibit specific shape-dependent properties and performances, since different crystallographic planes display different surface atomic structures.[1−5] Currently, realizing delicate control over the shape of nanocrystals is one of the hottest research subjects; researchers have devoted a great deal of effort to the shape control of nanostructures and the exploration of the shape−property relationship. For example, the antibacterial activities of micro/nanocrystals have been reported to depend greatly on the exposed crystal planes and can be tuned by the shape of the synthesized micro/nanocrystals.[6,7] Therefore, crystal shape design is essential for developing new micro/nanomaterials with high performance or unique applications. Up to now, simple metal oxide polyhedra with definite crystal planes, such as Cu_2O and Ag_2O, have been synthesized by various methods.[7,8] However, there are a few reports on shape control over complex metal oxides to control their properties, which might have a great deal of application potential in a variety of fields.

Zinc hydroxystannate ($ZnSn(OH)_6$), one of the most well-known complex metal hydroxides, has attracted extensive attention for its potential applications in many fields, such as flame retardant and smoke inhibitor[9] and photocatalyst.[10] Many methods, including coprecipitation approaches, solvothermal processes, wet sonochemical methods, and hydrothermal reactions, have been developed to prepare $ZnSn(OH)_6$ micro/nanocrystals in various shapes, such as cubes, hollow cubes, and octahedrons.[11−15] As known, $ZnSn(OH)_6$ is one of the perovskite oxides with face-centered-cubic (FCC) closed packing. Basically, an FCC crystal has a general sequence of surface energies, $\gamma\{111\} < \gamma\{100\} < \gamma\{110\}$ and the crystals are enclosed with {111} planes as the basal surfaces to

Received: July 10, 2012
Published: October 2, 2012

   dx.doi.org/10.1021/ic301496k | *Inorg. Chem.* 2012, 51, 10990−10995

Table 1. Sample Denotations, Their Corresponding Detailed Experimental Conditions, and Final Morphologies

	starting chemicals				
sample no.	$ZnAc_2{\cdot}H_2O$	$SnCl_4{\cdot}5H_2O$	MC (2.8 g/L)	NaOH	morphology
1	2 mL 0.5 M	2 mL 0.5 M	10	7 mmol	cubes
2	2 mL 0.5 M	2 mL 0.5 M	10	9 mmol	truncated cubes
3	2 mL 0.5 M	2 mL 0.5 M	10	13 mmol	cuboctahedrons
4	2 mL 0.5 M	2 mL 0.5 M	10	15 mmol	truncated octahedrons
5	2 mL 0.5 M	2 mL 0.5 M	10	17 mmol	octahedrons

minimize surface energy, while {100} or {110} lattice planes with relative high surface energies might grow faster and ultimately disappear during the crystal growth.[16] Some reports on the synthesis of cubic crystals bound by {100} lattice planes or octahedral crystals composed of the {111} lattice planes have been documented.[14,17] However there are few reports about the 14-faceted polyhedral crystals bounding with the {100} and {111} lattice planes with different ratios, not to mention the shape evolution from cubes to octahedrons. Since the conspicuous physical−chemical properties of nanostructures are sensitively correlated to their surface morphology, it is important to control the syntheses of the nanomaterials in order to provide different shapes for morphology−property investigations, especially under the same or similar conditions.[18−20]

In this study, we successfully controlled the crystallographic surface of $ZnSn(OH)_6$ crystals and systematically obtained $ZnSn(OH)_6$ in different shapes, including cubes, truncated cubes, cuboctahedrons, truncated octahedrons, and octahedrons using a simple solvothermal method in a methylcellulose (MC) ethanol/water solution. By adjusting the amount of the NaOH solution added to the reaction system, we first observed the shape evolution of $ZnSn(OH)_6$ particles from cube to octahedron with sizes gradually increasing from about 200 nm to 1−2 μm. These results not only provided the $ZnSn(OH)_6$ polyhedra with different lattice planes exposed, but also made it possible to investigate the morphology−property relationship of $ZnSn(OH)_6$ particles with different morphologies obtained under similar conditions. The antibacterial activities of the as-prepared $ZnSn(OH)_6$ polyhedral particles against *Escherichia coli* were studied and demonstrated to be surface-dependent. In addition, the cubic and octahedral Zn_2SnO_4/SnO_2 composites can be obtained by treating the $ZnSn(OH)_6$ cubes and octahedrons at 600 °C in the air.

EXPERIMENTAL SECTION

$ZnSn(OH)_6$ particles with different polyhedral shapes (i.e., cubes, truncated cubes, cuboctahedrons, truncated octahedrons, and octahedrons) were prepared using a facile one-pot solvothermal method. The synthetic process of cubic $ZnSn(OH)_6$ particles is described in detail as follows: Zinc acetate ($ZnAc_2{\cdot}2H_2O$, analytical grade) and tin tetrachloride ($SnCl_4{\cdot}5H_2O$, analytical grade) without further purification were used as starting materials. Methylcellulose (MC M450 chemically pure) was used as a crystal growth modifier. The MC was first dissolved in a 40% (v/v) ethanol/water solution. As in typical synthesis, 2 mL of 0.5 M $ZnAc_2$ solution and 2 mL of 0.5 M $SnCl_4$ solution were mixed under stirring to form a transparent solution, and then 2.3 mL of 3.0 M NaOH solution was added into the mixture to form a uniform suspension. After that, 10 mL of 2.8 g/L MC solution was added dropwise into the suspension. After stirring for 5 min, the mixture was transferred to and sealed in a 50-mL Teflon-lined autoclave, kept at 100 °C for 6 h, and finally cooled to room temperature. The precipitate was collected by centrifugation (4 000 rpm, 3 min), washed alternately with deionized water and ethanol, and air-dried at ambient conditions. The other polyhedral $ZnSn(OH)_6$ particles, including truncated cubes, cuboctahedrons, truncated octahedrons, and octahedrons, were prepared in a similar way except for difference of the amount of added NaOH solution. Table 1 lists the detailed synthetic conditions of various $ZnSn(OH)_6$ particles with different shapes, which are defined as samples 1−5 in order. For the synthesis of Zn_2SnO_4/SnO_2 composites, the obtained $ZnSn(OH)_6$ polyhedra were calcined in the air at 600 °C for 2 h and then cooled to room temperature naturally.

Characterizations. Powder X-ray powder diffraction (XRD) measurements were performed on a SHIMADZU XRD-6000 X-ray diffractometer with Cu Kα radiation (λ = 1.5418 Å) with 40 kV beam voltage and 30 mA beam current. The data were collected in the 10−70° range (2θ) with steps of 0.02°. Scanning electron microscopy (SEM) images were obtained on a Hitachi S-4800 field-emission scanning electron microscope. Transmission electron microscopy (TEM) images, high-resolution TEM (HRTEM) images, and the corresponding selected area electron diffraction (SAED) patterns were captured on the JEM-2100 transmission electron microscope at an acceleration voltage of 200 kV.

Antibacterial Tests. The antibacterial activities of the as-prepared cubic and octahedral $ZnSn(OH)_6$ particles were evaluated against *E. coli* ATCC8099 by plate count method. During the test with Luria−Bertani (LB)-agar plates, the prepared $ZnSn(OH)_6$ particles were uniformly distributed in water to form suspensions of various concentrations. Then 100 μL of aqueous suspensions was added into 20 mL of molten LB-agar solution. Subsequently, the mixture was poured into a Petri dish and cooled to solidify at room temperature to form an agar plate. Other agar plates with various concentrations were made in the same way, and each kind had three parallel samples. The agar plate without any particles added was also made as the control. Finally, 100 μL of suspensions of bacteria was inoculated on each LB-agar plate and incubated overnight in the dark at 37 °C. The inhibitory rate was used to evaluate the antimicrobial effect of particles, which is defined by the following formula.

$$\text{inhibitory rate\%} = \left(1 - \frac{\text{colony number of treated bacteria}}{\text{colony number of control bacteria}}\right) \times 100\%$$

RESULTS AND DISCUSSION

The $ZnSn(OH)_6$ particles were prepared with the assistance of MC under solvothermal conditions. Table 1 lists the experimental details for the $ZnSn(OH)_6$ with different morphologies, which are defined as samples 1−5. The crystalline phases of the obtained products were characterized by X-ray powder diffraction (XRD). The XRD patterns of the as-prepared $ZnSn(OH)_6$ particles are shown in Figure 1. All XRD diffraction peaks of the product can be indexed to a pure cubic perovskite $ZnSn(OH)_6$ (JCPDS: 73-2384); the sharpness of the peaks implies the high crystalline quality of the as-prepared sample. As the used amount of NaOH increases, the intensities of the XRD peaks increase, indicating that the addition of NaOH benefits the growth of $ZnSn(OH)_6$ crystal. Figure 2a shows a typical large-area SEM image of sample 1, indicating the presence of homogeneous, well-shaped nano-

dx.doi.org/10.1021/ic301496k | Inorg. Chem. 2012, 51, 10990−10995

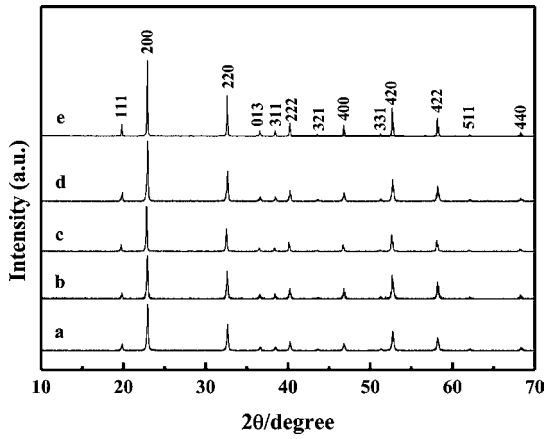

Figure 1. XRD patterns of the $ZnSn(OH)_6$ samples prepared with the addition of different amounts of NaOH: (a) 7 mmol, (b) 9 mmol, (c) 13 mmol, (d) 15 mmol, and (e) 17 mmol.

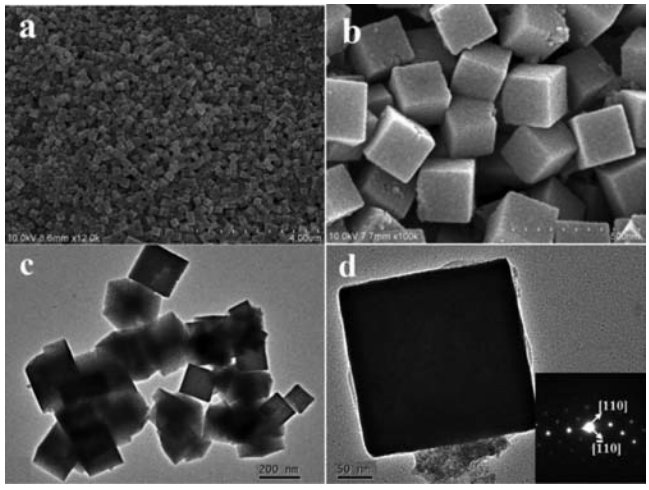

Figure 2. (a, b) SEM and (c, d) TEM images of $ZnSn(OH)_6$ cubes; Inset (d) SAED pattern of a single $ZnSn(OH)_6$ cube.

crystals with sizes of about 200 nm. As shown in the high-magnification SEM image (Figure 2b), the as-prepared nanocrystals are cubic. $ZnSn(OH)_6$ has an FCC cubic structure and as known by the three-dimensional (3-D) model (Figure 3a), the exposed surfaces of the cubes are made of six {100}

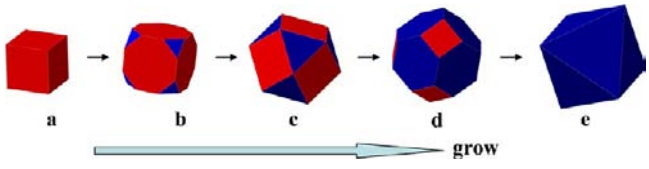

Figure 3. 3-D geometry models of the polyhedral crystals: the red facets represent {100} facets while the blue facets represent {111} facets.

facets. More structural information of the as-prepared $ZnSn(OH)_6$ polyhedra is provided by TEM characterizations. Figure 2c gives a typical low-magnification TEM image and also confirms that sample 1 is composed of cubic $ZnSn(OH)_6$ particles with sizes around 200 nm. As shown in Figure 2d, a single well-faceted cubic particle under an electron beam perpendicular to its top surface resembles a square. The corresponding selected area electron diffraction pattern (Figure 2d inset) presents a set of diffraction spots with a square symmetry, which can be indexed as the diffraction pattern of the [001] zone axis. It confirms the surfaces of the cubic $ZnSn(OH)_6$ particles are exposed with six equivalent {100} facets.

Figure 4a and b show SEM images of sample 2 prepared with 9 mmol of NaOH. Figure 4a shows the sample is still composed

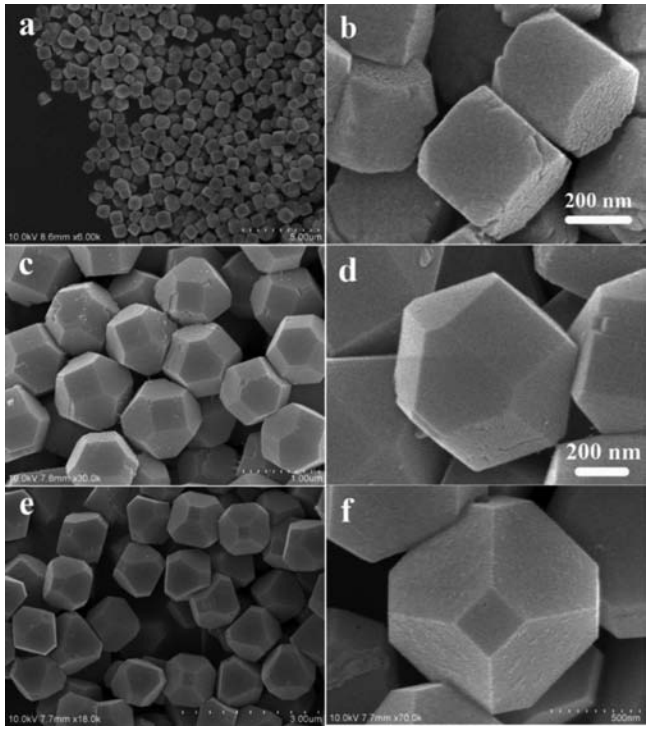

Figure 4. SEM images of (a, b) truncated cubes, (c, d) cubooctahedrons, and (e, f) truncated octahedrons.

of cubic nanocrystals. But Figure 4b, which uses a relatively higher magnification, shows these nanocubes are corner-truncated. As demonstrated by the three-dimensional (3-D) model (Figure 3b), the exposed surfaces of the truncated-cubes are made of six {100} facets with {111}-truncated surface. Increasing the amount of NaOH to 13 mmol, sample 3 proves to be composed of larger-sized cuboctahedrons as shown in Figure 4c and d. Further increasing the amount of NaOH results in the formation of $ZnSn(OH)_6$ octahedrons. When the amount of NaOH is increased to 15 mmol, the obtained sample 4 shows truncated octahedrons as shown in Figure 4e and f. When the amount of NaOH is increased to 17 mmol, the $ZnSn(OH)_6$ crystals are perfect octahedrons with point angles (Figure 5a and b). Figure 5c shows a typical low-magnification TEM image of octahedral $ZnSn(OH)_6$ particles with sizes around 2 μm. Most of the particles exhibit a diamond shape (Figure 5b) under the electron beam. Figure 5e and f show the HRTEM image and its FFT transformation, which demonstrate the single-crystalline nature of the cubic $ZnSn(OH)_6$ crystal. These results reveal that with the increase in the amount of NaOH, the products experience a shape evolution from cubes, to truncated-cubes, cuboctahedrons, truncated octahedrons, and finally to high symmetry octahedrons, corresponding to a progressive shrinkage of {100} and an enlargement of {111}, with sizes increasing as illustrated in Figure 3.

dx.doi.org/10.1021/ic301496k | *Inorg. Chem.* 2012, 51, 10990–10995

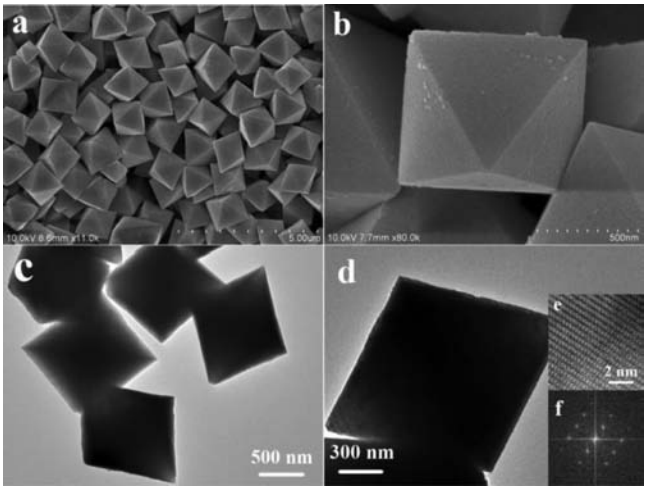

Figure 5. (a, b) SEM images, (c, d) TEM images, and (e, f) HRTEM image and its FFT transformation of $ZnSn(OH)_6$ octahedrons.

SEM observation of the products reveals that the amount of added NaOH is a key factor to control the morphology evolution of the obtained $ZnSn(OH)_6$ particles.The shape and size of the as-prepared $ZnSn(OH)_6$ polyhedral particles depend closely on the amount of NaOH added. As the amount of NaOH increases, the morphologies of the samples change from cube to octahedron with the increasing size. It is interesting to note that the shape and size of $ZnSn(OH)_6$ particles can be controlled only by adjusting the amount of NaOH present in the MC ethanol/water solution. It is therefore important to understand the formation of $ZnSn(OH)_6$ polyhedra. In this study, the level of NaOH-dependent morphology evolution of $ZnSn(OH)_6$ polyhedra can be explained by a mechanism in which $ZnSn(OH)_6$ particles with different morphologies are obtained by the following reaction:

$$ZnAc_2 + SnCl_4 + 6NaOH = ZnSn(OH)_6 + 4NaCl + 2NaAc$$

The above reaction suggests that the formation of different $ZnSn(OH)_6$ polyhedra is related to the concentration of the NaOH solution in the reaction system. By maintaining the concentrations of Zn^{2+} and Sn^{4+}, but changing the amount of NaOH, results in a change in the concentration of NaOH. In the experiments, if the amount of NaOH was 7 mmol for the synthesis of $ZnSn(OH)_6$ cubes, white precipitation was obtained when the NaOH was mixed with a solution of $ZnAc_2$ and $SnCl_4$, and the precipitation did not dissolve after stirring for 5 min. But if the amount of NaOH was 17 mmol for $ZnSn(OH)_6$ octahedrons, there was no precipitation existent. As known, the amount of NaOH can influence the kind of products for a direct reaction of Zn^{2+} and Sn^{4+} with OH^- ions. If the NaOH was not excessive, $Zn(OH)_2$ and $Sn(OH)_4$ were obtained, while if NaOH was excessive, $Zn[(OH)_4]^{2-}$ and $Sn[(OH)_6]^{2-}$ were obtained. The difference in the reaction between Zn^{2+} or Sn^{4+} with OH^- ions provides an opportunity to kinetically control the desired morphologies of $ZnSn(OH)_6$ polyhedral particles. When the NaOH concentration is low, the formation of the precipitation results in a low growth speed of $ZnSn(OH)_6$ nanocrystals, leading to the formation of $ZnSn(OH)_6$ cubes with a size of 200 nm and six equivalent {100} surface facets. With the increasing of the NaOH concentration, more and more of the precipitation dissolves to form $Zn[(OH)_4]^{2-}$ and $Sn[(OH)_6]^{2-}$. The reaction between $Zn[(OH)_4]^{2-}$ and $Sn[(OH)_6]^{2-}$ would no doubt be faster than the reaction between $Zn(OH)_2$ and $Sn(OH)_4$ precipitation. As $ZnSn(OH)_6$ nanocrystals grow faster, the {100} facets with relative higher surface energy also grow faster and would finally disappear. When the amount of NaOH is 17 mmol, the obtained $ZnSn(OH)_6$ nanocrystals are octahedrons with lower surface energy of {111} surface facets and with larger sizes of about 1−2 μm. To demonstrate that the growth of $ZnSn(OH)_6$ is related to the specific pH value, we also used ammonia as alkali source to control the morphology of $ZnSn(OH)_6$. However, with the addition of ammonia, only $ZnSn(OH)_6$ nanoparticles can be obtained as shown in Figure S1 (Supporting Information) and the morphologies of the samples can not be controlled by adjusting the ammonia amount. So, the morphology of $ZnSn(OH)_6$ is not just related to the specific pH values, but depend on the growth circumstance of different additives. Furthermore, the existences of MC and ethanol in the reaction system also have great effects on the morphologies of as-obtained products. Without the addition of ethanol and MC, the delicate control over the shape evolution of $ZnSn(OH)_6$ from cube to octahedron cannot be realized. The addition of ethanol changes the polarity of the system. MC would be adsorbed onto the $ZnSn(OH)_6$ surfaces; different surfaces would have different adsorption abilities to MC. Both of them would have the function to adjust the growth speed of $ZnSn(OH)_6$ nanocrystals, leading to the delicate control of $ZnSn(OH)_6$ shape evolution.

The antibacterial activities of the as-prepared $ZnSn(OH)_6$ polyhedral particles against *E. coli* were investigated by plate count method. In our studies, two typical polyhedral $ZnSn(OH)_6$ particles with cubic and octahedral morphologies (samples 1 and 5) were tested. Figure 6 displays the inhibitory

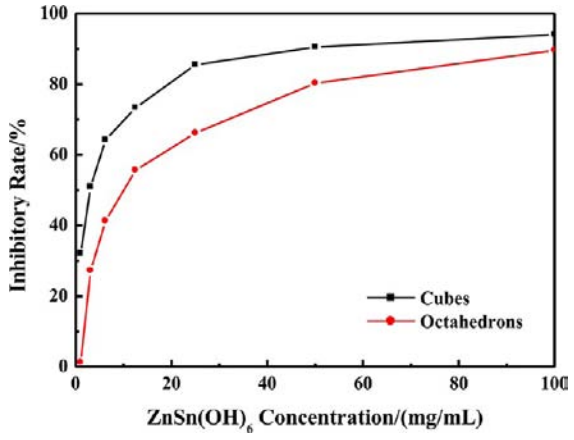

Figure 6. Inhibitory rates as a function of particle concentrations.

rates of two kinds of $ZnSn(OH)_6$ samples with different concentrations against *E. coli*. From it, it can be seen that both the cubic and the octahedral $ZnSn(OH)_6$ particles can efficiently inhibit the growth of *E. coli*, and their antibacterial abilities become stronger with increasing particle concentrations. The antibacterial effect of the cubic $ZnSn(OH)_6$ particles is better in comparison with that of the octahedral $ZnSn(OH)_6$ particles with the same concentration. Metals such as silver (Ag), gold (Au), copper (Cu), and zinc (Zn) are well-known for their antibacterial activities and are used for a number of in vitro and in vivo applications.[21] In our

experiments, the morphology-dependent antibacterial activities of $ZnSn(OH)_6$ polyhedral particles should originate from the exposed facets with different atomic arrangements, which might influence the release of Zn^{2+} ions from the crystal surface to the medium. The cubic and octahedral $ZnSn(OH)_6$ particles are bounded by the {111} and {100} facets, respectively. The surface energy of the {100} facets is higher than the {111} facets. As a result, the {100} facets are more reactive than the {111} facets, and by contrast Zn^{2+} ions are easily dissolved from the {100} facets.

The as-prepared $ZnSn(OH)_6$ polyhedra can also be used as precursors for Zn_2SnO_4/SnO_2 composites. Figure 7 displays

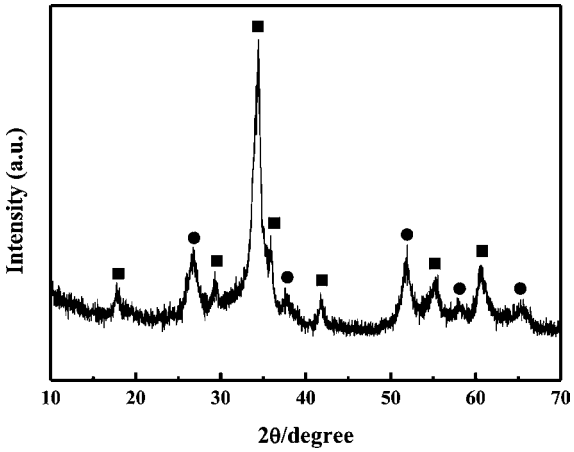

Figure 7. XRD pattern of the sample prepared by calcining $ZnSn(OH)_6$ cubes at 600 °C for 2 h.

the XRD pattern of the samples prepared by calcining the $ZnSn(OH)_6$ cubes in air at 600 °C for 2 h. The diffraction peaks marked "■" can be indexed to cubic Zn_2SnO_4 (JCPDS card: 24-1470) and the other diffraction peaks marked "●" can be indexed to tetragonal SnO_2 (JCPDS card: 41-1445), suggesting that Zn_2SnO_4/SnO_2 composites have been obtained. The process should go through the following reaction:

$$2ZnSn(OH)_6 \xrightarrow{600^\circ C} Zn_2SnO_4 + SnO_2 + 6H_2O$$

Figure 8 shows SEM and TEM images of the samples prepared by calcining the $ZnSn(OH)_6$ cubes and octahedrons. It can be clearly seen that both the samples keep the morphology of the precursors and $ZnSnO_4/SnO_2$ composites with cubic and octahedral structures have been successfully obtained, respectively.

CONCLUSIONS

In summary, we first observed the shape evolution of the complex metal oxide $ZnSn(OH)_6$ from cube to octahedron, with sizes gradually increasing from about 200 nm to 1−2 μm. The $ZnSn(OH)_6$ particles with different polyhedral shapes, including cubes, truncated cubes, cuboctahedrons, truncated octahedrons, and octahedrons were systematically synthesized via a simple solvothermal method at 100 °C in the presence of a methylcellulose (MC)/ethanol solution. This method not only allows the possibility to investigate the morphology−property relationship of $ZnSn(OH)_6$ particles with different morphologies obtained under similar conditions, but also might provide a general method to delicately control the shape evolution of other complex oxides. The antibacterial activity of

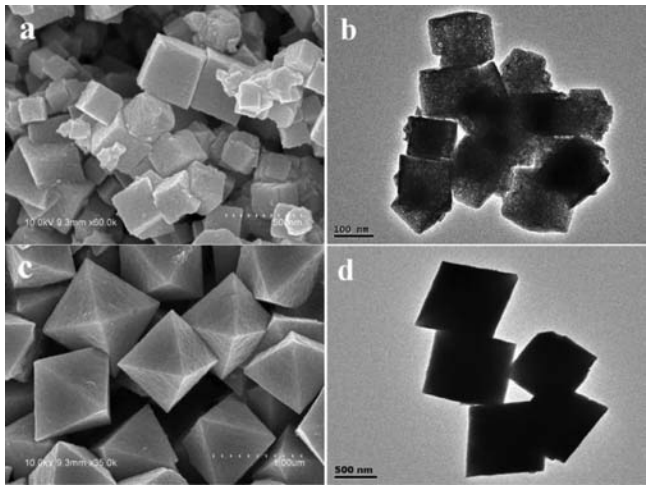

Figure 8. SEM and TEM images of the samples prepared by calcining the $ZnSn(OH)_6$ cubes and octahedra at 600 °C for 2 h.

the cubic $ZnSn(OH)_6$ particles is better in comparison with that of the octahedral $ZnSn(OH)_6$ particles with the same concentration. Additionally, cubic and octahedral Zn_2SnO_4/SnO_2 composites can be obtained by treating the $ZnSn(OH)_6$ cubes and octahedrons at high temperature in the air.

ASSOCIATED CONTENT

Supporting Information

SEM images of the obtained $ZnSn(OH)_6$ prepared with the addition of different amounts of ammonia solution. This material is available free of charge via the Internet at http://pubs.acs.org.

AUTHOR INFORMATION

Corresponding Author

*Email: fgao@nju.edu.cn (F.G.), qylu@nju.edu.cn (Q.L.).

Notes

The authors declare no competing financial interest.

ACKNOWLEDGMENTS

This work is supported by the National Basic Research Program of China (Grant 2011CB935800), the National Natural Science Foundation of China (Grants 21071076, 21021062, and 21201072), and the Natural Science Foundation of Jiangsu Province (Grants BK2010370 and BK2012241).

REFERENCES

(1) Xie, X. W.; Li, Y.; Liu, Z. Q.; Haruta, M.; Shen, W. J. *Nature* **2009**, *458*, 746.
(2) Geng, B. Y.; Fang, C. H.; Zhan, F. M.; Yu, N. *Small* **2008**, *4*, 1337.
(3) Leng, M.; Liu, M. Z.; Zhang, Y. B.; Wang, Z. Q.; Yu, C.; Yang, X. G.; Zhang, H. J.; Wang, C. *J. Am. Chem. Soc.* **2010**, *132*, 17084.
(4) Zhang, L. C.; Zhou, Q.; Liu, Z. H.; Hou, X. D.; Li, Y. B.; Lv, Y. *Chem. Mater.* **2009**, *21*, 5066.
(5) Han, X. G.; Jin, M. S.; Xie, S. F.; Kuang, Q.; Jiang, Z. Y.; Jiang, Y. Q.; Xie, Z. X.; Zheng, L. S. *Angew. Chem., Int. Ed.* **2009**, *48*, 9108.
(6) Pang, H.; Gao, F.; Lu, Q. Y. *Chem. Commun.* **2009**, 1076.
(7) Wang, X.; Wu, H. F.; Kuang, Q.; Huang, R. B.; Xie, Z. X.; Zheng, L. S. *Langmuir* **2010**, *26*, 2774.
(8) Zhang, D. F.; Zhang, H.; Guo, L.; Zheng, K.; Han, X. D.; Zhang, Z. *J. Mater. Chem.* **2009**, *19*, 5220.
(9) Cusack, P. A.; Hornsby, P. R. *J. Vinyl Addit. Technol.* **1999**, *5*, 21.

(10) Wang, L. L.; Tang, K. B.; Liu, Z. P.; Wang, D. K.; Sheng, J.; Cheng, W. *J. Mater. Chem.* **2011**, *21*, 4352.
(11) Basciano, L. C.; Peterson, R. C.; Roeder, P. L.; Swainson, I. *Can. Mineral.* **1998**, *36*, 1203.
(12) Fu, X. L.; Wang, X. X.; Ding, Z. X.; Leung, D. Y. C.; Zhang, Z. Z.; Lomg, J. L.; Zhang, W. X.; Li, Z. H.; Fu, X. Z. *Appl. Catal., B* **2009**, *91*, 67.
(13) Jena, H.; Kutty, K. V. G.; Kutty, T. R. N. *Mater. Chem. Phys.* **2004**, *88*, 167.
(14) Yu, X. J.; Lu, H. X.; Li, Q.; Zhao, Y. L.; Chen, D. L.; Fan, B. B.; Wang, H. L.; Yang, D. Y.; Xu, H. L.; Zhang, R. *Cryst. Res. Technol.* **2011**, *46*, 1079.
(15) Qin, Z.; Huang, Y. H.; Wang, Q. Y.; Qi, J. J.; Xing, X. J.; Zhang, Y. *CrystEngComm* **2010**, *12*, 4156.
(16) Wang, Z. L. *J. Phys. Chem. B* **2000**, *104*, 1153.
(17) Wrobel, G.; Piech, M.; Dardona, S.; Ding, Y.; Gao, P. X. *Cryst. Growth Des.* **2009**, *9*, 4456.
(18) Peng, X.; Manna, L.; Yang, W.; Wickham, J.; Scher, E.; Kadavanich, A.; Alivisatos, A. P. *Nature* **2000**, *404*, 59.
(19) El-Sayed, M. A. *Acc. Chem. Res.* **2001**, *34*, 257.
(20) Jiao, S. H.; Xu, L. F.; Jiang, K.; Xu, D. S. *Adv. Mater.* **2006**, *18*, 1174.
(21) Schrand, A. M.; Rahman, M. F.; Hussain, S. M.; Schlager, J. J.; Smith, D. A.; Syed, A. F. *Nanomed. Nanobiotechnol.* **2010**, *2*, 544.